Journal of Magnetic Resonance 236 (2013) 134–139

Contents lists available at ScienceDirect

Journal of Magnetic Resonance

journal homepage: www.elsevier.com/locate/jmr

Communication

Stabilization of the inverse Laplace transform of multiexponential decay through introduction of a second dimension

Hasan Celik, Mustapha Bouhrara, David A. Reiter, Kenneth W. Fishbein, Richard G. Spencer *

Laboratory of Clinical Investigation, National Institute on Aging, National Institutes of Health, Baltimore, MD 21224, USA

ARTICLE INFO

Article history:
Received 17 May 2013
Revised 9 July 2013
Available online 24 July 2013

Keywords:
Inverse problems
NMR relaxometry
Fredholm integral

ABSTRACT

We propose a new approach to stabilizing the inverse Laplace transform of a multiexponential decay signal, a classically ill-posed problem, in the context of nuclear magnetic resonance relaxometry. The method is based on extension to a second, indirectly detected, dimension, that is, use of the established framework of two-dimensional relaxometry, followed by projection onto the desired axis. Numerical results for signals comprised of discrete T_1 and T_2 relaxation components and experiments performed on agarose gel phantoms are presented. We find markedly improved accuracy, and stability with respect to noise, as well as insensitivity to regularization in quantifying underlying relaxation components through use of the two-dimensional as compared to the one-dimensional inverse Laplace transform. This improvement is demonstrated separately for two different inversion algorithms, non-negative least squares and non-linear least squares, to indicate the generalizability of this approach. These results may have wide applicability in approaches to the Fredholm integral equation of the first kind.

Published by Elsevier Inc.

1. Introduction

An important type of 1-dimensional NMR transverse relaxometry yields time-domain data of the form [1]:

$$y(t) = \int_0^\infty F(T_2) e^{-t/T_2}\, dT_2 \tag{1}$$

describing a superposition of signals relaxing independently, with $F(T_2)$ the weight of the component with decay constant T_2. Data would typically be acquired by sampling the echo maxima of a Carr–Purcell–Meiboom–Gill (CPMG) pulse sequence. Eq. (1) has the form of a Laplace transform, and extraction of $F(T_2)$ via the inverse Laplace transform (ILT) is a classically ill-posed problem [2,3]. We demonstrate that the recovery of $F(T_2)$ from $y(t)$ is stabilized when a second, indirect, dimension, is introduced. We show this in the context of NMR experiments, in which two-dimensional relaxometry and related experiments are already well-established.

Ill-posedness renders the result of the ILT highly sensitive to noise and of potentially limited accuracy. Regularization reduces, but does not render insignificant, these limitations [4]; in addition, the derived $F(T_2)$ is highly sensitive to the degree of regularization [5]. Similar comments apply to other uses of the ILT to derive distributions of, for example, longitudinal relaxation time, T_1, and diffusion coefficient, D.

2-Dimensional (2D) relaxometry experiments in NMR yield time domain data of the form:

$$\tilde{y}(\tilde{t}, t) = \int_0^\infty \int_0^\infty F(T_1, T_2) e^{-\tilde{t}/T_1} e^{-t/T_2}\, dT_1\, dT_2, \tag{2}$$

where we have used T_1, and T_2 as the variables in the separable exponential kernel for illustrative purposes. This form of the T_1 dependence can be achieved by subtracting the signal obtained for a given inversion time $\tilde{t}$ from the signal obtained using $\tilde{t} \gg T_1$. Signal-to-noise ratio (SNR) for simulations and experiments was defined after this subtraction.

Expressions of identical form apply to other 2-dimensional relaxometry and hybrid experiments involving, e.g. the pairs (T_2, T_2), and (T_2, D) [1,6,7]. In each case, a pulse sequence incorporating an indirectly-detected dimension with variable evolution time $\tilde{t}$, or, e.g., an incremented gradient, and a directly-acquired dimension parameterized by time is implemented. Through consideration of previous results on the stability of the ILT [2], and the fact that the span of multiplicatively separable functions mapping $\mathbb{R}^2 \to \mathbb{R}^1$ is dense in the set of all such functions, we hypothesized that the 2D ILT would display greater accuracy and stability with respect to noise than the 1D ILT. Experiments yielding expressions of the form of Eq. (2) could then be used to determine $F(T_2)$ through projection of the two-dimensional ILT onto the T_2 axis (Fig. 1).

The goal of the present work is to demonstrate that deriving the 1D ILT via the 2D ILT, that is, the path defined by the solid arrows in Fig. 1, yields much-improved results as compared to the direct calculation of the 1D ILT, that is, the dashed arrow path. We will refer

* Corresponding author. Fax: +1 410 558 8318.
E-mail address: spencerri@mail.nih.gov (R.G. Spencer).

1090-7807/$ - see front matter Published by Elsevier Inc.
http://dx.doi.org/10.1016/j.jmr.2013.07.008

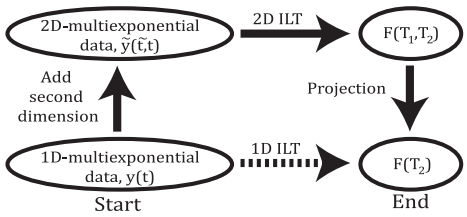

Fig. 1. Dashed arrow indicates the 1D ILT of multicomponent decay data consisting of decaying exponentials, resulting in a T_2 histogram. The path traversed by the solid arrows introduces a second dimension to the data with a distinct, indirectly-sampled time variable $\tilde{t}$, representing, e.g. the inversion time in a T_1 measurement. The T_2 histogram is then obtained by applying a 2D ILT to the two-dimensional data and then projecting the resulting T_1–T_2 histogram onto the T_2 axis.

to the 2D method as 2D ILT projection (2D ILTP). Because ILT results improve with greater SNR, the comparison between the 1D and 2D approaches must be made on an equal-time basis. In the 2D experiment, acquisition time is proportional to the number of rows of data, m, acquired in the indirect dimension. Applying this additional time instead to signal-averaging a 1D acquisition would result in a $\sqrt{m}$ increase in SNR. Therefore, we compare results from a 2D dataset with results from a 1D dataset having a factor $\sqrt{m}$ higher SNR, or, equivalently, compare 1D to 2D experiments conducted with equal total acquisition time, where the repetition time was set to five times the T_1 of the slowest decaying component.

Simulation results, and experimental data from agarose gel phantom samples, will be presented. Two established methods for carrying out the ILT of a signal exhibiting multiexponential decay, non-negative least squares (NNLS) and non-linear least squares (NLLS), were investigated to determine the generalizability of our analyses. NNLS has the significant advantage of not requiring pre-specification of the number of underlying exponentials. In contrast, with NLLS, data points are fit to a pre-specified non-linear model function, which in our case is the sum of two decaying exponentials. Thus, NLLS requires a careful selection of signal model and reasonable initial estimates for fit parameters. NNLS suffers from much greater numerical instability and generally requires regularization to achieve reliable results. In addition, the flexibility of the NNLS approach leads to much more stringent SNR requirements for stability and accuracy as compared to NLLS. Finally, even for a signal generated by two discrete relaxation components, regularized NNLS will return a histogram of T_2 values that may or may not resolve these components. In contrast, NLLS, by definition, returns and therefore resolves the number of components incorporated into the model, whether or not this accurately represents the system under study.

2. Methods

For NNLS, Eq. (1) was discretized with $K-1$ permissible log-spaced values of T_2 and N time-domain data points

$$y(t_n) = \sum_{k=1}^{K-1} F(T_{2,k}) e^{-t_n/T_{2,k}} + C, \tag{3}$$

where $y(t_n)$ is the amplitude of the nth echo and $F_k = F(T_{2,k})$ is the unknown T_2 distribution to be derived in the form of $K-1$ weights. This equation is discretized with A_{nk} as the $N \times K$ matrix representing the integral equation kernel. The final column accounts for a possible signal offset C. Thus, $A_{nk} = e^{-t_n/T_{2,k}}, k \leqslant K-1$, $A_{nK} = 1$, and the final entry in F is $F_K = C$. A Tikhonov regularization term controlled by the parameter μ was added in the usual manner [3,4], so that the target function used for minimization with NNLS took the form:

$$X = \sum_{n=1}^{N} \left\| \sum_{k=1}^{K} A_{nk} F_k - y_n \right\|^2 + \mu \left\| \sum_{k=1}^{K} F_k \right\|^2 \tag{4}$$

This approach was extended in the conventional fashion for the two-dimensional relaxometry experiments defined by Eq. (2) [6]. We selected the value of μ so that regularization increased the misfit to the data

$$\chi^2 = \sum_{n=1}^{N} \sum_{k=1}^{K} \frac{(A_{nk} F_k - y_n)^2}{\sigma^2} \tag{5}$$

exhibited by the unregularized version of Eq. (4), that is, omitting the second term, by 1% [8]. Here, σ is the standard deviation (SD) of the noise in the data as determined after complete signal decay.

For NLLS, a two-component signal model consistent with the experimental data was assumed:

$$y(t_n) = M_0 \left(f_1 e^{-t_n/T_{2,1}} + f_2 e^{-t_n/T_{2,2}} \right) + \epsilon \tag{6}$$

for 1D relaxometry, and

$$\tilde{y}(\tilde{t}_m, t_n) = M_0 \left(f_1 e^{-t_n/T_{2,1}} e^{-\tilde{t}_m/T_{1,1}} + f_2 e^{-t_n/T_{2,2}} e^{-\tilde{t}_m/T_{1,2}} \right) + \epsilon \tag{7}$$

for 2D. Here, the f_i are component fractions satisfying $f_1 + f_2 = 1$, $T_{1,i}$ and $T_{2,i}$ are relaxation time constants, M_0 is the signal amplitude and ϵ represents additive Gaussian noise.

Numerical data, including those in plots, are presented as mean ± SD, except that error bars in Fig. 4 are standard error of the mean (SEM).

3. Simulation results

Simulation and experimental results were obtained using a value of $m = 6$ for the number of points sampled in the indirect dimension for the 2D analysis. This was selected based on a Cramer–Rao lower bound calculation [9–11] (see supporting information), which indicated marginal further improvement in results for $m > 6$.

The sensitivity of the ILT to noise [2] is illustrated in Fig. 2. There is clearly a large variation in the morphology of the derived T_2 histogram from the 1D ILT (Fig. 2a); in fact, the two underlying signal components are resolved in only five out of the 12 noise realizations. Fig. 2b shows the results of the 2D analysis performed on an equal-time basis through adjustment of SNR. Both components are cleanly resolved for all noise realizations and component amplitudes are much more stable than in Fig. 2a. Similar results were obtained for the much more challenging problem of analysis of three underlying relaxation components with relaxation times and weights given by (T_2, weight) = (7 ms, 5%), (12 ms, 5%) and (50 ms, 90%) for 1D, and with T_1 values of 300 ms, 600 ms and 1500 ms incorporated for each component respectively in 2D. Again, resolution was consistently observed using the 2D approach but not with the 1D analysis, and quantification was much more accurate with 2D ILTP (data not shown).

Using NNLS, we systematically investigated the reliability of 2D ILTP for resolving two closely-spaced relaxation components with the same signal parameters as in Fig. 2. Results for a range of SNR values were obtained for 100 realizations of noise; components were considered resolved if the minimum of the T_2 distribution lying between the components was less than 90% of the amplitude of the smaller component. SNR values were incremented until the two components were consistently resolved. For the 1D ILT, SNR = 25,000 was required in order that the components were resolved for 90% of the noise realizations (Fig. 3a), while a much more modest SNR ~ 700 was required for the 2D approach (Fig. 3b). For the equal time comparison, the 1D ILT with

Download English Version:

https://daneshyari.com/en/article/5405572

Download Persian Version:

https://daneshyari.com/article/5405572

Daneshyari.com